

General Disclaimer

One or more of the Following Statements may affect this Document

- This document has been reproduced from the best copy furnished by the organizational source. It is being released in the interest of making available as much information as possible.
- This document may contain data, which exceeds the sheet parameters. It was furnished in this condition by the organizational source and is the best copy available.
- This document may contain tone-on-tone or color graphs, charts and/or pictures, which have been reproduced in black and white.
- This document is paginated as submitted by the original source.
- Portions of this document are not fully legible due to the historical nature of some of the material. However, it is the best reproduction available from the original submission.

X-661-75-115
PREPRINT

NASA TM X- 70894

Si (Li) X-RAY ASTRONOMICAL SPECTROSCOPY

(NASA-TM-X-70894) Si (Li) X-RAY ASTRONOMICAL
SPECTROSCOPY (NASA) 28 p HC \$3.75 CSCL 03B

N75-23924

Unclas
G3/35 21711

STEPHEN S. HOLT

MAY 1975



————— **GODDARD SPACE FLIGHT CENTER** —————
GREENBELT, MARYLAND

Si(Li) X-Ray Astronomical Spectroscopy

Stephen S. Holt

Abstract: The general considerations involved in the choice of Si(Li) as a non-dispersive spectrometer for x-ray astronomy are discussed. In particular, its adaptation to HEAO-B is described as an example of the space-borne application of Si(Li) technology.

Paper presented at the

Symposium on the Techniques of
Solar and Cosmic X-Ray Spectroscopy

Mullard Space Science Laboratory

May 1975

The resolving power of dispersive x-ray technology is so clearly superior to that obtainable with non-dispersive devices that considerable effort has been expended during the last decade to apply this resolution advantage to X-ray astronomy. A variety of dispersive instruments have been proposed for space flight, and a few have already been configured into spacecraft payloads.

There still remains, however, sufficient impetus not only to continue non-dispersive x-ray astronomical spectroscopy at its present level of sophistication, but also to develop new non-dispersive spectroscopic tools. The reason for this apparent lack of foresightedness is simply the relative inefficiency of dispersive techniques, because X-ray astronomy will always be a quantum-limited discipline. Even in the case of HEAO-B, the large orbiting grazing-incidence x-ray telescope to be launched in 1978, dispersive spectroscopy can be considered practical for only the very strongest sources, and will probably be used for only a few percent of the totality of targets observed by the telescope.

If very sharp features in cosmic spectra are present, dispersive spectroscopy is absolutely essential in the determination of line and edge profiles. There are, however, good theoretical reasons for believing that line features in typical x-ray sources will be broadened¹ in excess of not only the resolution of Bragg spectrometers, but in excess of their rocking curves, as well. Such broadening makes the detection of such features virtually impossible with crystals or gratings.

Non-dispersive spectrometers, capable of viewing the entire spectrum simultaneously with high efficiency, can study these broadened features

as well as continua, and perform spectral-temporal correlations in fluctuating sources. If their resolving power can be increased above what is normally available in a proportional counter, they may even have a detection capability for narrow features comparable with (or even better than) dispersive techniques (i.e. in the same accumulation time). The reasons why Si(Li) is the preferred non-dispersive spectrometer for this application are a combination of its inherent resolution advantages², and its adaptability to the constraints and philosophy of the HEAO-B observatory.

A non-dispersive spectrometer, in principle, is nothing more than a finite volume of matter. The first condition is that this matter be cold enough so that it is not completely ionized. This is because the detection of incident radiation is accomplished via the separation of charge, and the recognition of this charge component as a signal characteristic of the incident radiation. In the case of incident charged particles, a trail of detached electrons are created directly in the Coulomb path of the particles. For incident neutral radiation, there must be an auxiliary step in the charge creation process. In the x-ray energy range of interest here, the only significant channel for the creation of charge is through direct photo-electric interaction with the detection medium. The resultant photo-electrons and Auger electrons are then detected as though these electrons were primary incident charged particles. At high photon energies, Compton and pair-production effects may be important in the initial charge creation.

If we attempt to make a useful detector out of a solid, we can appreciate almost immediately that the material must be neither a good insulator nor a good conductor. An insulator will prevent the collection of the charge that is separated by the incident radiation, and a conductor will prevent the identification of the charge as freshly created and separate from the sea of conduction charge available. A useful device, therefore, must be semiconducting, in the sense that putting a bias across the detector will enable created charge to be collected before it recombines or is trapped, without a steady current saturating the charge collection device. Ordinary semi-conducting materials (Si and Ge) are not really good enough, although high-purity Ge is now commercially available with low enough bulk resistivity to make a good detector. The technology of solid state detectors is devoted to making what amounts to such "perfect" semi-conductors, and the prime technique is the use of reverse-biased p-n junctions.

Pure semi-conducting materials are simple crystals with band gaps between the valence and conduction bands of the order of one volt. For pure silicon, where the band gap is 1.2V, there are $\sim 10^{10}$ conduction band electrons cm^{-3} at room temperature (i.e., the bulk resistivity is much too low to operate usefully). Lowering the temperature helps dramatically, so that a low operating temperature will always be prescribed no matter what other improvements can be made. "Doping" the crystal with atoms which replace occasional Si atoms in the lattice is the now traditional way to make a semi-conductor worse before it can be made better. In "n-doping", each impurity atom contributes an extra valence electron (relative to Si), which is so loosely bound to the lattice that it is,

effectively, an extra conduction band electron. Such a material has a much lower bulk resistivity than does pure Si. Similarly, "p-doping" is done with impurities which lack an electron per atom in the lattice, and the lattice "hole" moves analogously to a positive conduction electron. The great advantage of doping in this application is, like in the case of solid-state electronic devices, when a reverse-biased p-n junction is employed.

As illustrated in Figure 1, the unbiased diode will have a surplus of electrons on the n-side, and a surplus of holes on the p-side. Applying an electric field in the direction shown moves the majority carriers in each segment away from the junction, so that the central portion of the composite crystal is "depleted" of carriers. This means that the depleted region is an insulator in the sense that the steady-state flow of current is extremely low, however the carrier mobility is high enough so that any charge created via the ionization losses of incident charged particles can be swept out and collected at the ends.

As a practical matter, we can make the dead (non-depleted) layer on one end very low by using a wafer which is p-doped, for example, and diffusing a thin n-layer on one end. The dead layer on the n-side when bias is applied can generally be kept to ~ 0.1 micron. This is important, of course, if the detector is required to have high efficiency for x-rays.

Even with a thin dead layer on the front face of the detector, such a "surface barrier" reverse-biased p-n junction detector will have a depleted thickness of no more than ~ 1 mm, as the junction will break down at some limiting bias value. A thicker depleted layer is useful for at least two reasons: a larger active detector volume, and a lower detector

capacitance. A technique which has been useful in increasing the depletion-layer thickness is lithium drifting, whereby extremely precise compensation for the acceptor concentration in p-type material may be obtained from the use of lithium as a mobile donor.³ Thicknesses of $> 1\text{ cm}$ are possible with drifted devices.

In considering the better semiconductor for application to x-ray spectroscopy (i.e. silicon or germanium), silicon is clearly favored. The prime reason is its lower atomic number, which enables the sustenance of a relatively transparent window at the surface. This also means less contamination from the interaction of higher energy photons which deposit only a fraction of their energy into the separated charge. Si is also easier to handle than Ge, as lithium-drifted Si crystals are stable enough so that they can be temperature-cycled, while a Ge crystal will lose its lithium compensation when taken to room temperature. The only possible advantage which Ge might have over Si is in ultimately achievable resolution, and this is by no means certain.

The reason why Ge may be an inherently higher resolution device is because its band gap is less than that of Si, so that, in principle, more charge may be separated for the same amount of ionization. The ultimately achievable resolution of any device is determined by the variance in the number of primarily separated charge, so that a low value of ϵ (energy required to produce an ion pair) is important; it is not, however, the whole story. There is the competing process of energy loss to the medium, and the division between created charged and such energy loss is, like the number of charges created, a statistical process.

If the yield (y) is defined as the number of separated ions for a given amount of energy deposition (E), then

$$y = E/\epsilon.$$

If there was no competing loss to the medium, the variance (σ^2) of the yield would be trivial (i.e. the resolution of the detector would be virtually perfect). This should not be confused with the situation where a charged particle passes through a detector, depositing an amount of energy with some variance of its own. In the case of a detected photon, there is a precise total energy deposition E . If the competing loss to the medium dominates (so that the probability for ion separation is small), the variance in y should be strictly Poisson. These, and all intermediate cases, may formally be parameterized by the postulation of a "Fano factor" (F) which is the ratio of the variance σ^2 to the yield, with F ranging between zero (for the case of perfectly efficient charge separation) and unity (for the case of highly inefficient charge separation)⁴. Clearly, the important quantity to minimize is not ϵ , but the product ϵF . Although ϵ is lower for Ge than for Si, it is not clear which has the lower product ϵF .

It is useful, at this point, to consider the limiting resolution possible with a Si(Li) detector if charge separation were the only relevant consideration. Using $\epsilon = 3.81\text{eV}$ and $F \approx 0.1$, the FWHM resolution at $\sim 1\text{ keV}$ would be

$$\text{FWHM} = 2.355 \sqrt{\epsilon F E} = 46\text{ eV}.$$

For a proportional counter, the corresponding resolution would be, since $\epsilon \sim 30\text{eV}$ and $F \sim 1$, $\Delta E \approx 400\text{eV}$ (and, for the sake of completeness, if $F \sim 1$ for Si, the FWHM resolution would be $\sim 145\text{eV}$). In fact, the presently

possible Si(Li) resolution at 1 keV is closer to the $F \sim 1$ case, but the statistics of charge separation have nothing to do with our inability to achieve better resolution. The problem is in the extraction of the charge, not in its production. Experimentally and theoretically, F for Si is within a factor of 2 of .1^b.

The great advantage offered by proportional counters is the low-noise amplification of the primarily created charge in the counter itself. Unfortunately, solid state detectors with such internal amplification have not yet been developed, so that the x-ray resolution limit is presently determined by the noise in the electronics used to extract the signal from the detector. There are several specific causes for this electronic noise,⁶ some of which can be controlled. The basic limitation is the thermal noise generated in the conducting channel of the FET used as the input amplifying element of the charge amplifier. It is crucial, therefore, that the FET used has been specially selected for low noise characteristics. The traditional way to represent this noise component is in terms of equivalent noise charge (ENC), i.e. the amount of charge required to produce a signal equivalent to this noise. As the effect of the FET noise can be idealized as an equivalent noise resistance R_s in series with the gate, the FET noise can be written

$$\overline{(ENC)}_s = \sqrt{4.2 kTR_s \frac{C_{in}^2}{\tau}}$$

where k is the Boltzmann constant, T is the absolute temperature, C_{in} the input capacitance (farads), and τ is a filtering time constant (seconds). The coefficient is determined by the impulse response of the filter, which we have assumed here to be gaussian (τ is the FWHM, not the sigma of the

gaussian).

The best presently available FET's are 2N4416, for which noise decreases with temperature as indicated above down to $\sim 130^\circ$, but then worsens at lower temperatures. With a typical limiting value of $TR_g \sim 4.1 \times 10^4$ ohm $^\circ$ K, we obtain

$$FWHM_g = 2.355 e \frac{ENC_g}{e} \approx 85 \frac{C'_{in}}{\sqrt{\tau'}} \text{ eV}$$

where e is the electronic charge, C'_{in} in measured in picofarads and, τ' is measured in microseconds. Clearly, we can optimize the resolution by minimizing the input capacitance and maximizing the integration time. Even with a detector contribution to the capacitance which is of the order of 1pf, the internal capacitance on the FET gate must be at least a few pf, so that it is not possible to attain less than ~ 100 eV noise contribution from the FET unless the integration time is $> 10 \mu\text{sec}$, giving ~ 25 eV/pF.

This means that conventional amplification techniques are going to degrade the resolution of the system still more, as the feedback resistor R_f used to drain the charge is a noise source in parallel with the input. This noise contribution is given by

$$ENC_p = \sqrt{1.5KT \frac{\tau}{R_f}}$$
$$FWHM_p = 2.8 \times 10^9 \sqrt{\frac{\tau}{R_f}}$$

(τ in seconds, R_f in ohms). As the feedback resistance is practically limited to $\sim 5 \times 10^9$ ohms (since the real component of resistance decreases with frequency independent of the DC resistance, and the only resistance which matters is at the filter frequency), this noise source has a contribution comparable to the FET noise at $\tau \sim 10 \mu\text{sec}$. Even worse, this noise contribution increases if we increase the filter time constant. It

is for this reason that opto-electronic feedback must be used⁷, which eliminates this noise source completely. The charge balance at the input is maintained by the periodic application of light to the FET junction. This produces a current which flows from the drain to the gate, (i.e. opposite to that from collected charge) so that the input can be thus discharged without an external resistance. The light is triggered from a light-emitting diode which operates by sensing the input bias: when a present level is reached, the system is disabled, the LED pulsed, and then the system is restored to operational status. This bias can be conveniently set to > 1 MeV charge deposition, in which case a detector leakage current of $\sim 10^{-14}$ amps alone would require such a discharge every ten seconds or so. The total system disable time at each discharge is < 100 msec.

With the resistor noise removed, it would seem that increasing the integration time can continue to better the resolution. The very best resolutions obtained in the laboratory (~ 100 eV) have utilized integration times $\sim 100\mu$ sec, but there are two remaining noise limitations which compromise the practicality of such large integration times. $1/f$ noise in lossy dielectrics represents an asymptotic limitation, and leakage current shot noise and (especially) microphonism will have increased noise contributions with larger time constant. Therefore, we cannot expect that integration times as large as 100μ sec will be practical in space flight applications.

With the aforementioned as a general (albeit cursory) background, we can begin to discuss the development of the space-borne non-dispersive spectrometer in detail. Si(Li) is the preferred medium, and an active

area of $\leq 30\text{mm}^2$ with a depleted depth of $\sim 3\text{mm}$ assures a capacitance sufficiently low to be smaller than the intrinsic and stray capacitance at the FET gate. The image of a point source at the focus of the HEAO-B telescope should be less than 0.1mm in extent, and the telescope pointing should be good to $\sim 1\text{mm}$. In order to be sure that the image is contained entirely on the active surface of the detector, we prefer to keep the detector area large (i.e. as large as the $\sim 6\text{mm}$ diameter of the $\sim 30\text{mm}^2$ detector) for three reasons: we can measure spectra from objects as much as a few arc minutes in size (like the Crab Nebula) calorimetrically, we can allow reasonable tolerances in assembly, and we can purposely defocus in order to minimize surface irregularities.

Figure 2 is the calculated efficiency for such a detector with nominal values of dead silicon and gold. A similar device has successfully measured K_{α} from Boron fluorescence in the laboratory². The x-ray port to the detection volume is through the gold p-contact, and it is expected that the system flown aboard HEAO-B will have very similar parameters. One problem with a gold layer this thin is its irregularity³. For the thicknesses $\leq 100 \text{ \AA}$, the evaporant is completely clumped and filamentary, so that an "average" thickness is virtually meaningless (i.e. at low energies, a more relevant parameter would be the open area between filaments, regardless of the filament thickness)¹⁰. At several hundred angstroms the gold is not yet truly uniform, so that even detectors with broad-beam responses must be well-calibrated. As the present application would use an area of $\leq 10^{-2}\text{mm}^2$ for the entrance port to x-rays from a point source if placed exactly at the focus, it is clear that some diffusion over a larger fraction of the detector face is desirable to minimize the effect of surface irregularities. The anticipated defocussing is planned to be

to a size of $\sim 1\text{mm}^2$, which should satisfy both the surface irregularity and pointing considerations.

In most applications, the high efficiency of the device will assure a relatively contamination-free spectrometer. Nevertheless, there will be instances near the quantum limitation of the spectrometer where active anti-coincidence would be desirable. We are attempting to provide this active anti-coincidence in two parts, one of which is included on the Si(Li) chip, itself. A standard technique in the manufacture of such devices is the machining of a groove on the n-side of the crystal to separate the depleted region from the residual non-compensated p-type silicon at the crystal periphery. This groove then allows the crystal to approximate the "top-hat" crystal geometry (where all the uncompensated material is cut away except for a thin rim on the metalized p surface), for which the limiting resolution has been obtained in the laboratory. There are two distinct advantages which can be obtained by placing a second groove inside the outer groove, and operating this annulus as a detector, itself. First, the inner groove defines a much sharper central volume edge, because there is no longer any adjacent field-free region if the annulus is biased (i.e. the field lines at the Au front surface of the detector will be much closer to perpendicular to this surface than they would be without the groove). Second, the annular volume can be operated in anti-coincidence with the central volume, so that any events which share charge with the annular volume can be eliminated. This removes not only charged particles which just graze the central volume from contaminating the spectrum, but also x-rays which convert at the very edge of volume and are inefficiently collected. Such a "guard ring" detector does

not significantly differ in limiting resolution (in principle) from a standard device¹¹, so that these two advantages would seem well worth the adaptation of this technique to our application.

The second anti-coincidence feature is the presence of a high-purity Ge "backstop" crystal. Its purpose is to anti-coincidence those charged particles which travel along the groove (and which the annular detector may not record), as well as serving as a partial anti-Compton suppressant, and a local monitor of the radiation background environment. A schematic of this composite detector assembly is shown in Figure 3.

A negative bias of $\sim 1000V$ is applied to the front (Au) face of the crystal, which is shared by both the central and annular detectors. The bare FET and LED are encapsulated in a header which is in close proximity to the low voltage end of the central volume, where the signal is extracted. The FET draws $\sim 20mW$, and is left on all the time so that its temperature can be kept close to optimum (which is higher than the temperature at which the whole assembly is kept). The header is light-tight to prevent the light from reaching the crystal directly, and the FET contact is through a thin low-thermal- conductivity gold wire.

The ring (annular) detecting volume utilizes high-resistance feedback on the FET charge loop, and both this FET and the feedback resistor are also contained within the detector assembly. In the final design, the components for both portions of the Si(Li) chip are mounted on a single boss which connects from the side, rather than having the series-mounting arrangement implied by Figure 3.

The germanium preamp is mounted outside of the assembly, and operated at ambient temperature. The anticipated noise component of the resolution of each detector is expected to be:

- (1) $\leq 120\text{eV}$ for the central Si(Li) volume
- (2) $\leq 250\text{eV}$ for the Si(Li) annulus
- (3) $\leq 2\text{keV}$ for the Ge(HP).

It is important to note that the effective low energy threshold for such a system is determined completely by the noise component of the resolution. Unlike the proportional counter case, where the low energy threshold can generally be set an order of magnitude above the noise level because the resolution is determined by the charge collection statistics, in this application we will attempt to get as close to the noise level as we can. As the $\sim 120\text{eV}$ above is a FWHM value, it corresponds to a gaussian σ of $\sim 50\text{eV}$ equivalent. Clearly the assumption of a white noise spectrum prescribes a minimum low energy threshold of a few hundred eV in order to be sure that all detected photons are real. As a practical matter, $\sim 400\text{eV}$ would seem to be an ideal threshold in terms of both the noise and the detector efficiency, but the situation is complicated somewhat by timing requirements. The experiment has several modes of output, some of which are generated simultaneously. These include:

- (1) Best possible spectral resolution of the x-rays detected in the central Si(Li) volume
- (2) Best possible spectral resolution of the x-rays detected in the annular Si(Li) volume
- (3) Best possible temporal resolution of the x-rays detected in the central Si(Li) volume.

Unfortunately, (1) and (3) are mutually exclusive, because (1) requires an integration time of tens of microseconds, and (3) requires an integration time no more than $\sim 1 \mu\text{sec}$. Because this experiment has high efficiency, we desire the capability of resolving photons with $\sim \mu\text{sec}$ separation in order to study burst phenomena in sources such as Cyg X-1¹². We also have to consider the fact that sources like Sco X-1 would saturate our system, and integration times as long as $\sim 100 \mu\text{sec}$ will leave us completely dead during the exposure because pile-up effects will anti-coincidence out everything.

For these reasons, there are three separate ranges of time constants selectable on the central Si(Li) detector. For spectroscopy, we select either the longest possible ($> 20 \mu\text{sec}$) or, if the counting rate is too high, a faster time constant ($\sim 4 \mu\text{sec}$). At the same time, a very fast ($\sim 1 \mu\text{sec}$) time constant is used for event detection (i.e. timing, with similarly fast time constants on the guard ring and Ge anti-coincidence). It must be remembered that the noise contribution to the energy resolution of this channel is ~ 5 times higher than that for $> 20 \mu\text{sec}$ shaping, so that its low energy threshold must be higher, as well. A block diagram for the front-end operation of the experiment in a mode where only central Si(Li) events would be recorded is illustrated in Fig. 4. The details of the logic strategy are a bit complicated, but relatively straightforward, and will not be discussed here.

The detector assembly shown schematically in Fig. 3 must be kept cold ($\approx 120^\circ$) in order to achieve the specified resolution. This is accomplished by placing the detector assembly in a cryostat. For HEAO-B, it is impractical to consider cooling passively or thermo-electrically, and the only

remaining possibility is a space-borne cryostat. The selected cooler is a two-stage methane-amonia system, which shares its vacuum with the detectors. The removable portion of the cryostat which includes the detector assembly (actually, two of them, with one in standby redundancy) is called the detector container, which is schematically illustrated in Fig. 5. The top of the detector container is at ambient spacecraft temperature ($\sim 300^\circ\text{K}$), and has a vacuum cover which can open in orbit. The cover has Fe^{66} sources mounted so that they can be viewed by the detectors when the cover is over them. The detectors, and the system end-to-end, can be calibrated in orbit with these sources and with on-board pulse generators.

Should the vacuum in the spacecraft be worse than the $\sim 10^{-8}$ torr anticipated, the detectors and the cryostat lifetime may suffer from this contamination. The cover will, therefore, be latchable in orbit in the event that contamination is noted. Should the contamination be so severe that the detector surface leakage increases, the detector assembly can be "defrosted" via heaters inside the cryostat. The design lifetime of the cryostat is two years.

A very thin window is placed just below the vacuum cover, which serves two purposes. It is designed to be a highly reflective surface to minimize radiation heat input to the cryostat, and to protect the detectors from the UV and optical radiation focussed by the telescope. It has a thickness of $\sim 1000\text{\AA}$, and is composed of Al vacuum-deposited on a parylene substrate. It is pressure relieved so that it is not a vacuum seal, and will not frost over since it is kept at ambient temperature.

The Be collimator below the window likewise serves two purposes. It is an effective x-ray baffle for low energy x-rays generated via fluorescence

in the cryostat, and is an effective cold trap for contaminants entering through the window. It is sunked to the secondary cryogen, at a temperature of $\sim 160^\circ\text{K}$. The detector container baseplate, to which the detector assembly attaches, is sunked to the primary refrigerant at a temperature of $\sim 100^\circ\text{K}$.

All the analog circuitry is attached directly to the top of the cryostat, with a completely digital interface to the rate accumulators, memory, command and formatting electronics which are configured elsewhere on the satellite, as indicated in Figure 6. The cryostat is shock-mounted to the turntable containing each of the instruments which take their turn at the telescope focus. The resonant frequency of the cryostat is $\sim 55\text{Hz}$, which should be low enough to prevent the coupling of mechanically induced microphonics into the system.

The HEAO-B satellite is scheduled for launch in 1978. With an effective collecting area of the order of 1000 cm^2 , it will enable the Si(Li) spectrometer to operate usefully between the detector-limited low energy threshold of $\sim 400\text{eV}$ and the high energy telescope cutoff at $\sim 4\text{keV}$. Figure 7 illustrates the approximate instrument 5σ sensitivity to hydrogenic K-lines from even-Z elements, as a function of observing time. Detector efficiency, system resolution, telescope through-put and relative abundance have been included properly, but the model input spectrum has been idealized to a very hot optically thin continuum on which hydrogenic emission lines are the only features. The overall spectroscopy capability of the entire observatory is even more powerful, as focal-plane Bragg spectrometry and objective grating spectrometry are also included in the instrumentation. Astronomical X-ray spectroscopy will make a great leap forward with the

launch of HEAO-B, and the complementarity of the dispersive and non-dispersive techniques employed will assure a set of spectroscopic tools available which are sufficiently general to cope with the surprises that we can expect this new level of sensitivity to furnish.

Acknowledgements

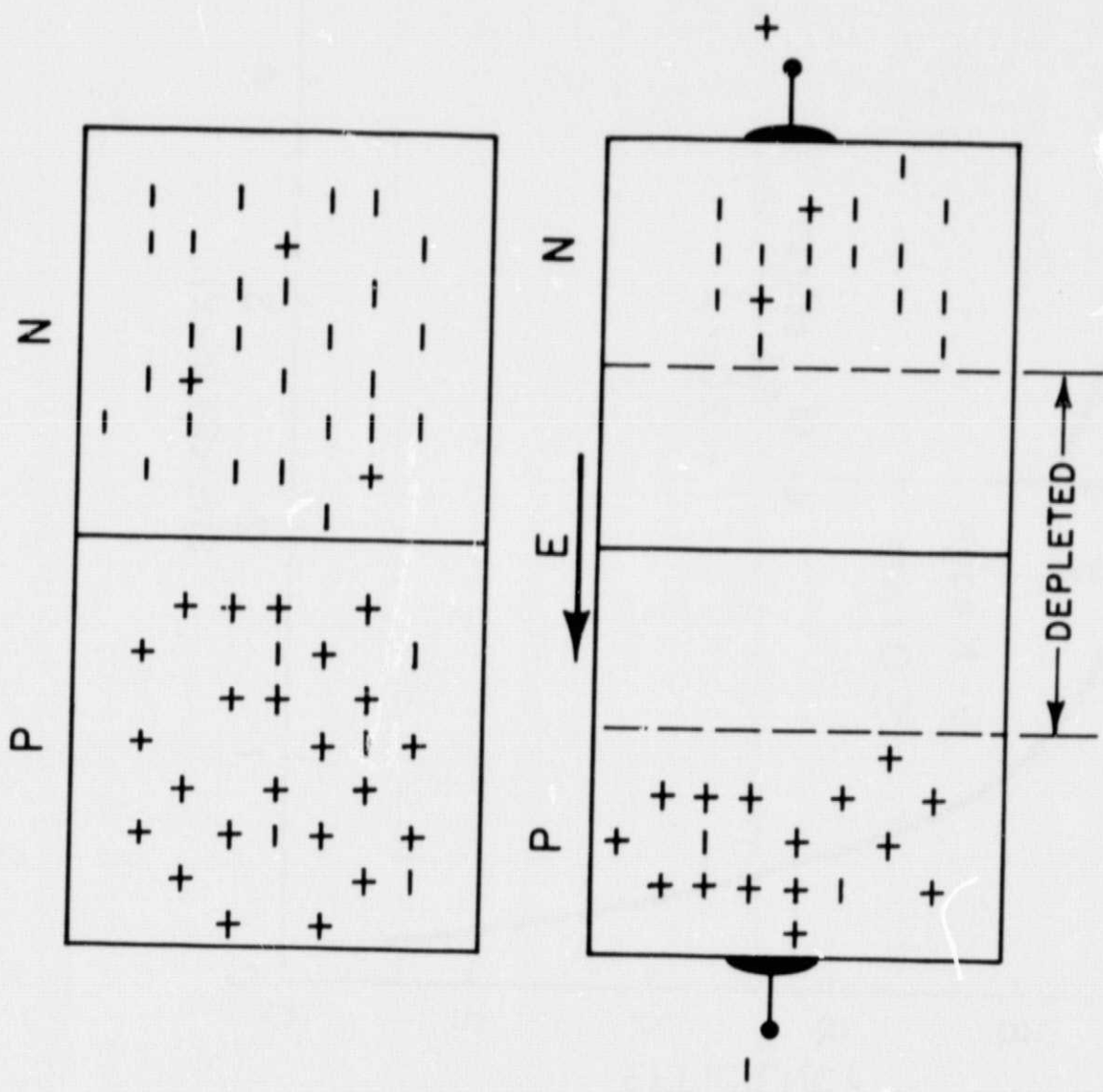
There are many scientists at the four institutions constituting the HEAO-B consortium (Columbia Astrophysics Laboratory, Goddard Space Flight Center, Massachusetts Institute of Technology and Smithsonian Astrophysical Observatory) who have contributed to the conception of this and the other experiments which comprise the observatory instrumentation. Special thanks are due Drs. H. Kraner and V. Radeka of the Brookhaven National Laboratory for their assistance in the development of the solid-state spectrometer.

References

1. J. E. Felten, M. J. Rees and T. F. Adams, *Astron. & Astrophys.* 21, 139 (1972)
2. A. H. F. Muggleton, *Nucl. Instr. & Meth.* 101, 113 (1972)
3. E. M. Pell, *J. App. Phys.* 31, 291 (1960)
4. U. Fano, *Phys. Rev.* 72, 26 (1947)
5. H. R. Zulliger and D. W. Aitken, *IEEE Trans. Nucl. Sci.* NS-17, 197 (1970)
6. V. Radeka, *Nucl. Instr. & Meth.* 99, 525 (1972)
7. D. A. Landis, F. S. Goulding and J. M. Jaklevic, *Nucl. Instr. & Meth.* 87, 211 (1970)
8. R. G. Musket, *Nucl. Instr. & Meth.* 117, 385 (1974)
9. K. L. Chopra, *Thin Film Phenomena*, McGraw Hill (1969)
10. J. M. Jaklevic and F. S. Goulding, *IEEE Trans. Nucl. Sci.* NS-18, 115 (1971)
11. J. M. Jaklevic and F. S. Goulding, *IEEE Trans. Nucl. Sci.* NS-19, 384 (1972)
12. R. E. Rothschild, E. A. Boldt, S. S. Holt and P. J. Serlemitsos, *Ap. J.* 189, L13 (1974)

Figure Captions

- (1) Idealization of a reverse-biased p-n junction detector. The application of reverse-bias results in a central region depleted of majority carriers which has low leakage current but high carrier mobility.
- (2) Calculated broad-beam x-ray efficiency of a Si(Li) detector with a dead window of Au and Si as indicated.
- (3) Schematic of the geometry in the HEAO-B solid-state detector assembly.
- (4) Block diagram of the primary logic mode of the HEAO-B solid-state spectrometer.
- (5) Schematic of the detector container, which is the plug-in module to the cryostat containing all detector-peculiar elements (including all electrical leads to the outside).
- (6) Schematic of the entire solid-state spectrometer experiment as configured on the HEAO-R satellite.
- (7) Approximate 5σ sensitivity to narrow K-emission lines from even-Z elements in a typical HEAO-B observation. Representative sources are indicated on the ordinate based upon their nominal source strength only.



ORIGINAL PAGE IS
OF POOR QUALITY

Fig. 1

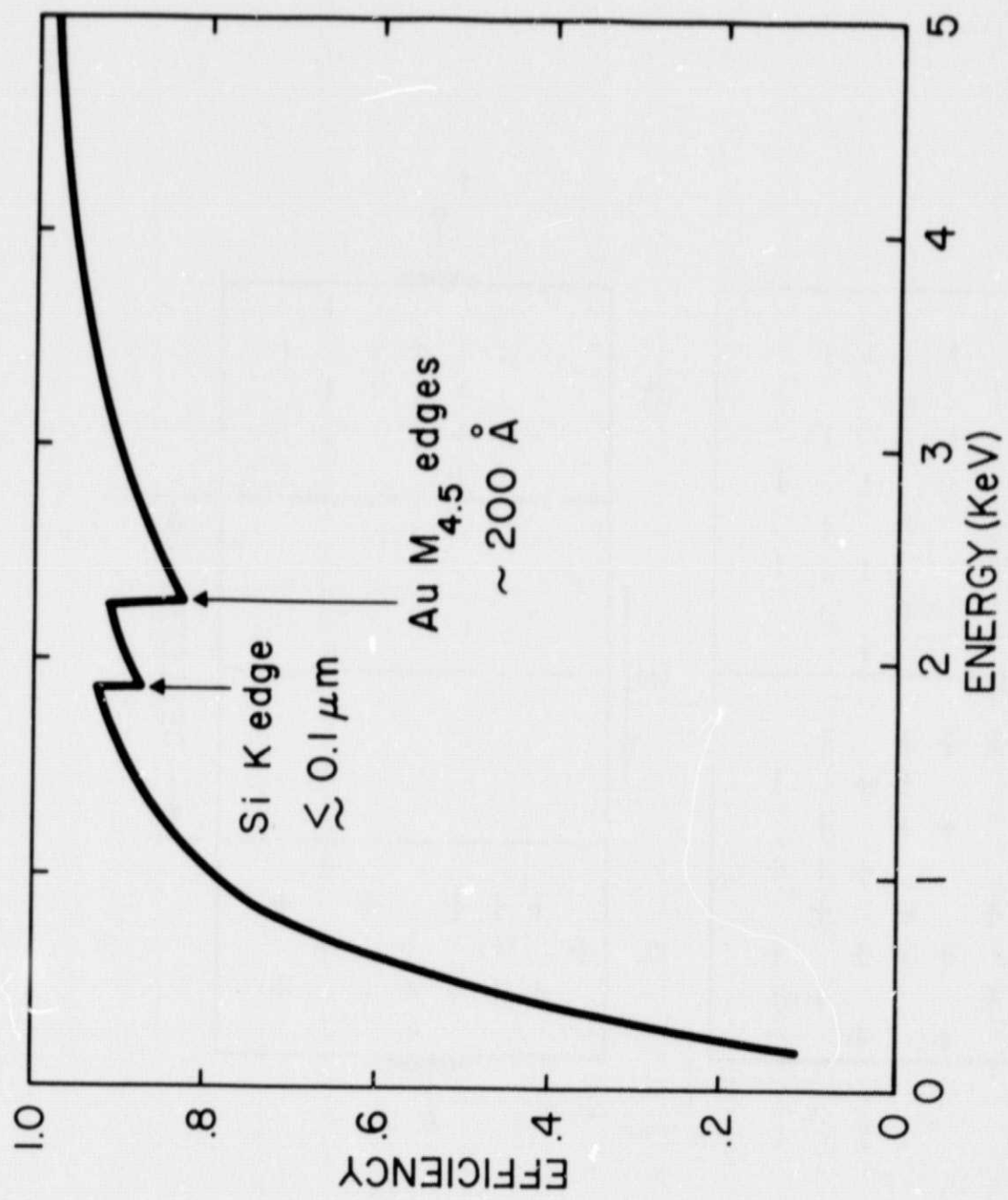
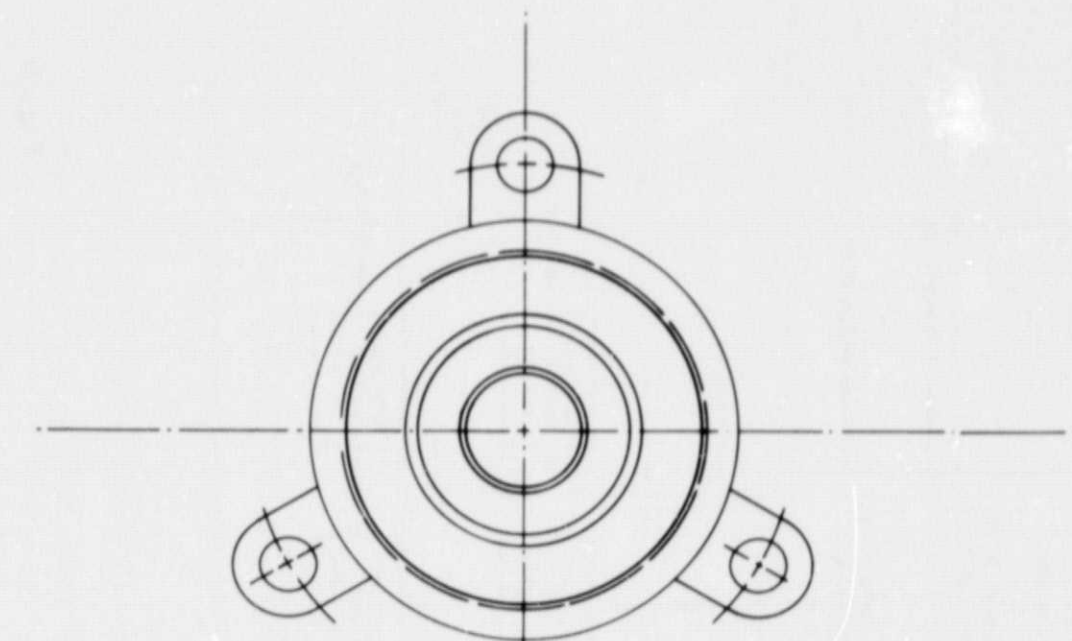

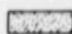


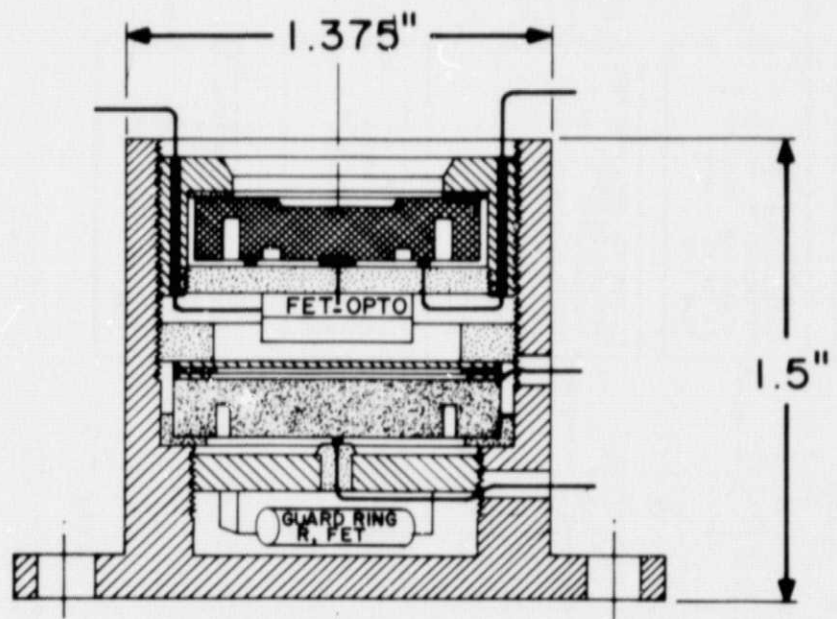


Fig. 2



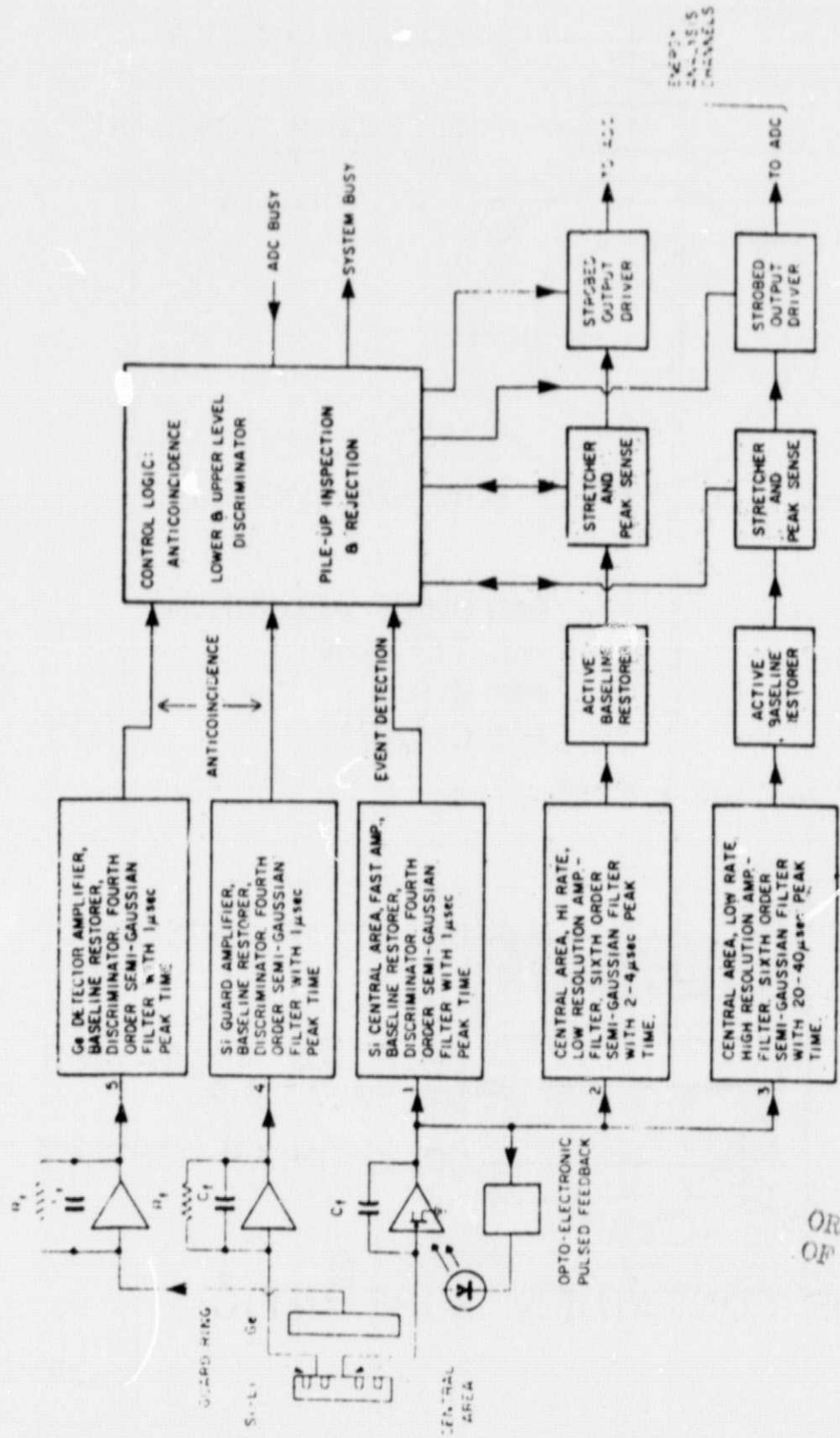
DETECTOR
ASSEMBLY

-  PURE ALUMINUM
-  TEFLON
-  Si(Li)
-  Ge(HP)



ORIGINAL PAGE IS
OF POOR QUALITY

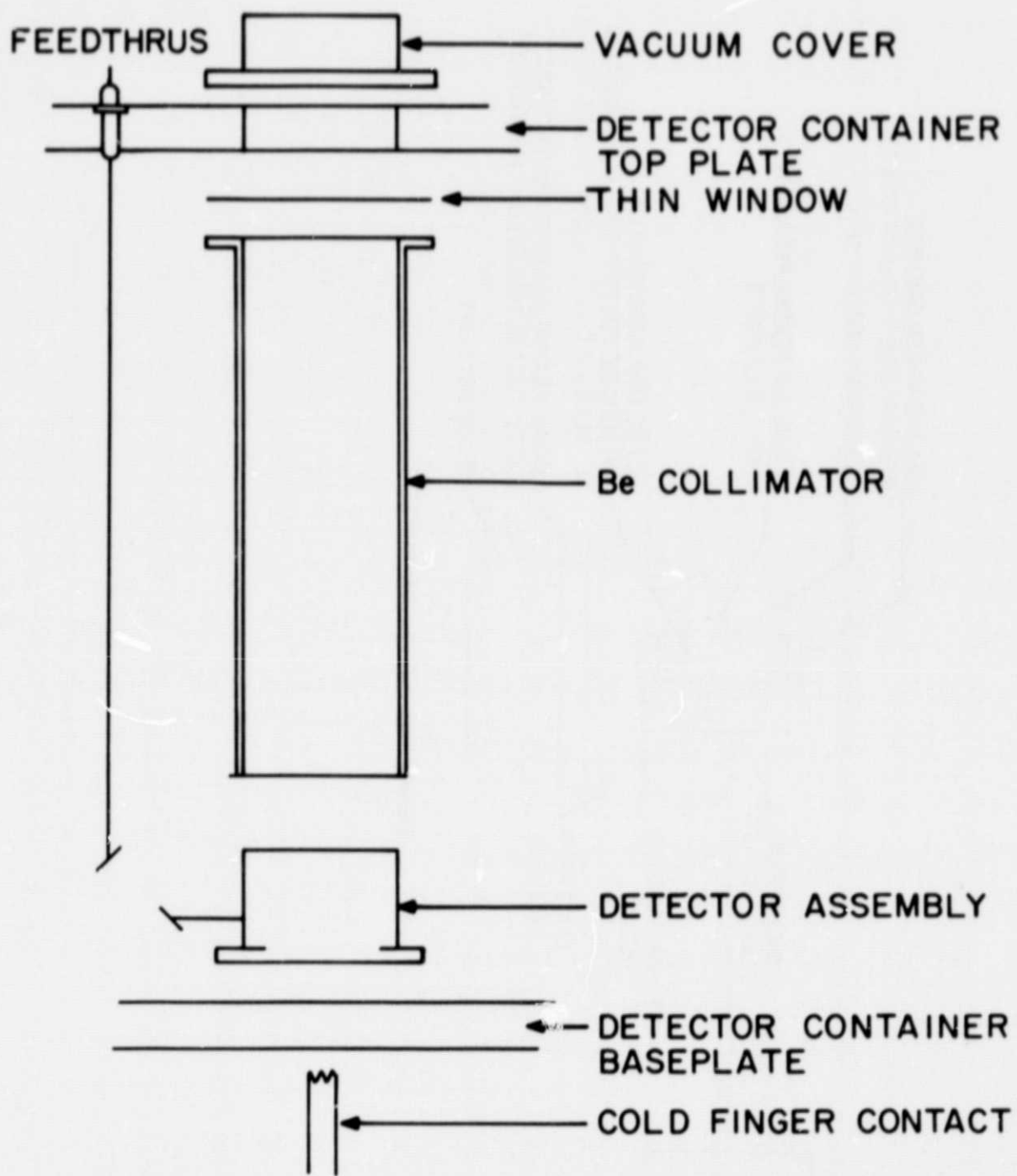
Fig. 3



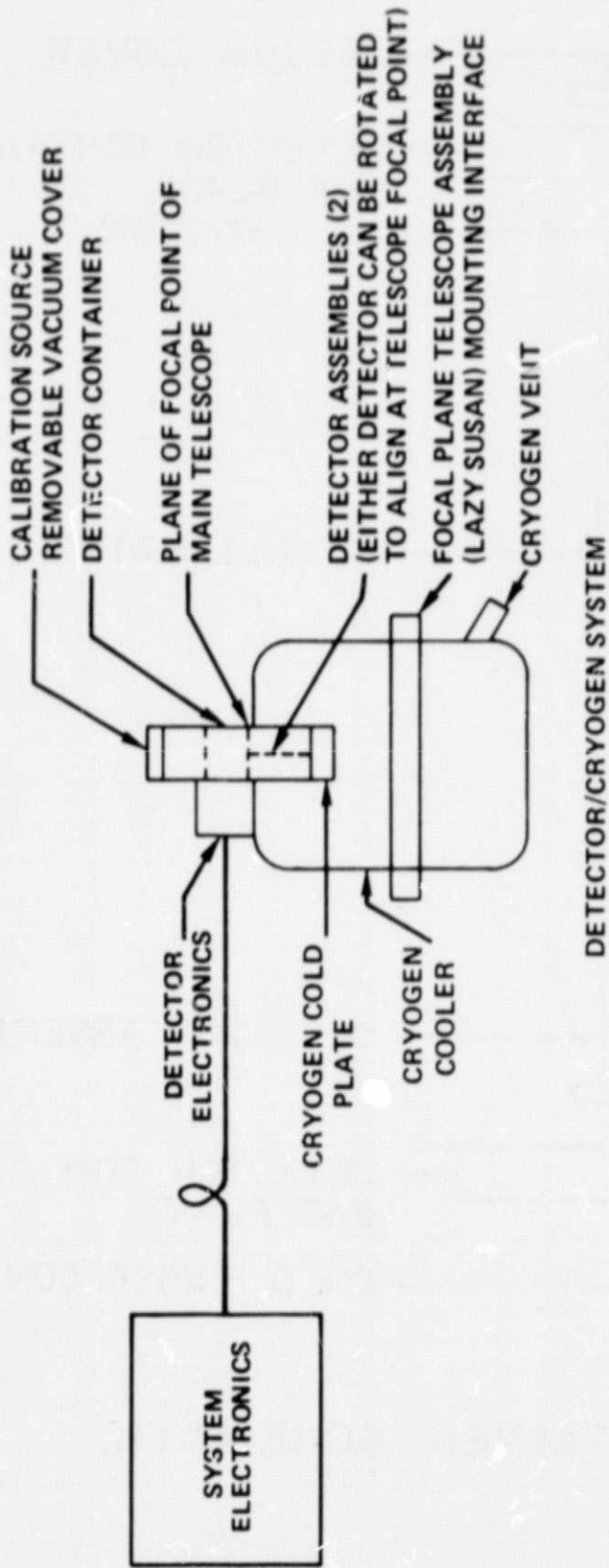
EVENTS
CHANNELS

Fig. 4

ORIGINAL PAGE IS
OF POOR QUALITY



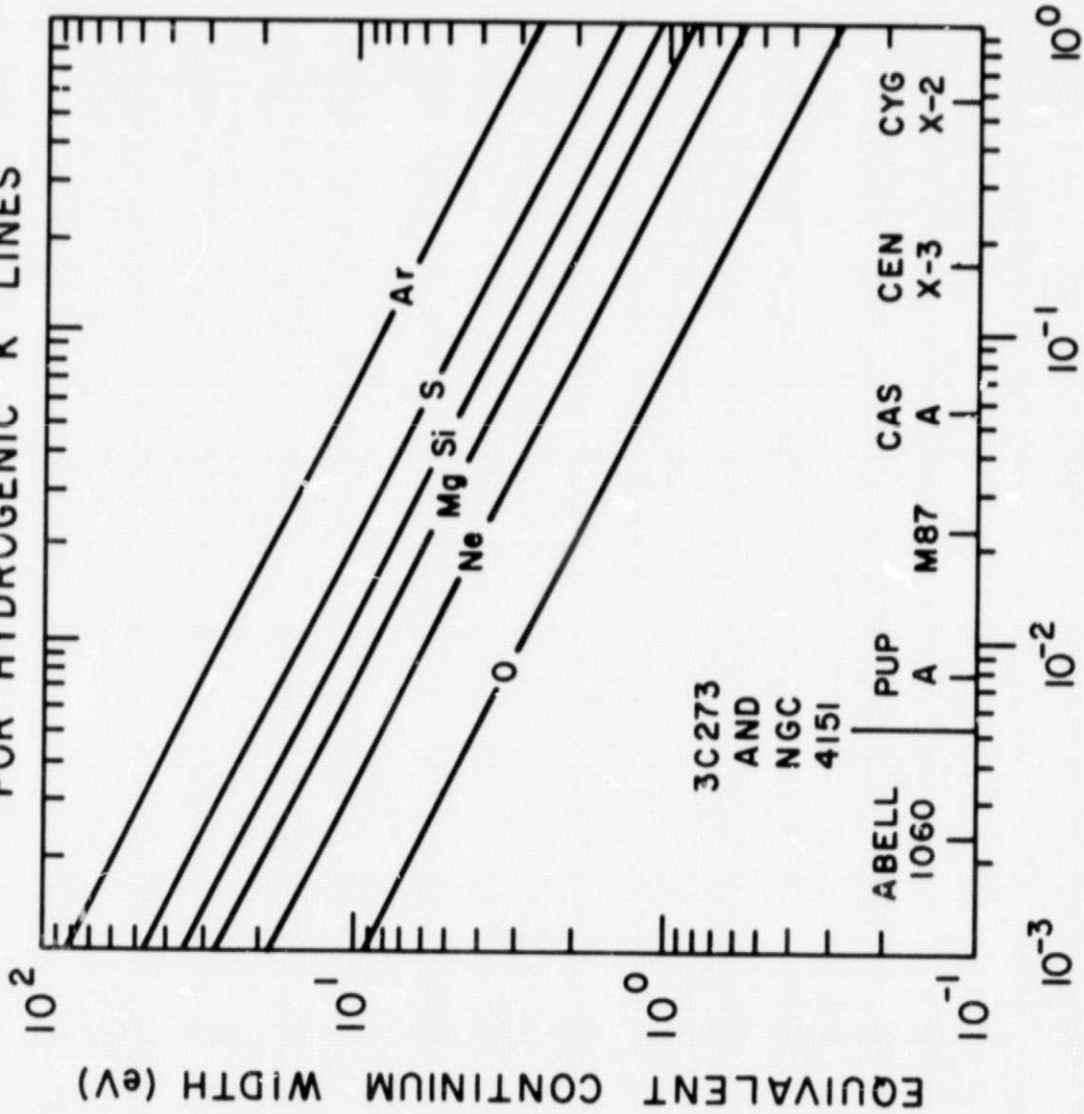
DETECTOR CONTAINER SCHEMATIC



ORIGINAL PAGE IS
OF POOR QUALITY

Fig. 6

DETECTION IN 1800 SEC (1/3 ORBIT)
FOR HYDROGENIC K LINES



SOURCE STRENGTH (FRACTION OF CRAB NEBULA)
FROM 3U CATALOG

Fig. 7